

Article

Aging-Related Changes in Expression and Function of Glutamate Transporters in Rat Spinal Cord Astrocytes

Shiksha Sharan ^{1,2,*}, Bhanu Prakash Tewari ^{1,3}  and Preeti G. Joshi ¹

¹ Department of Biophysics, National Institute of Mental Health and Neurosciences, Hosur Main Road, Bangalore 560029, India; bptewari@gmail.com (B.P.T.); joshipree@gmail.com (P.G.J.)

² Department of Psychiatry, National Institute of Mental Health and Neurosciences, Hosur Main Road, Bangalore 560029, India

³ Department of Neuroscience, University of Virginia, Charlottesville, VA 22903, USA

* Correspondence: shikshasharan1@gmail.com

Abstract: Astrocytes make up the predominant cell population among glial cells in the mammalian brain, and they play a vital role in ensuring its optimal functioning. They promote neuronal health and survival and protect neurons from glutamate-induced excitotoxicity. In the spinal cord's dorsal horn (DH) and ventral horn (VH) regions, astrocytes serve crucial roles. Notably, VH motor neurons exhibit a heightened sensitivity to glutamate-induced damage. It is posited that this selective sensitivity could be related to their localized presence within the VH, where astrocytes possess a distinct set of mechanisms for managing glutamate. As organisms age, the risk of damage from glutamate increases, indicating a potential decline in the efficiency of astrocytic glutamate regulation. Our research involved an analysis of astrocytic structure, glutamate transporter levels, and glutamate uptake capabilities within the DH and VH through immunohistochemical methods, protein analysis via Western blot, and patch-clamp studies in electrophysiology. The investigations revealed a decrease in both the number and coverage of astroglia in the spinal cord, more so within the VH as aging progressed. Notably, levels of the excitatory amino acid transporters 1 and 2 (EAAT1 and EAAT2) also decreased with age, particularly within the VH. Patch-clamp analyses of astrocytes from both spinal regions confirmed a significant reduction in glutamate uptake activity as age advanced, indicating an age-related impairment in glutamate processing. The findings indicate aging leads to distinct changes in DH and VH astrocytes, impairing their glutamate management abilities, which could contribute significantly to the development of late-onset neurodegenerative conditions.

Keywords: astrocytes; excitotoxicity; aging; glutamate; transporter; spinal cord



Citation: Sharan, S.; Tewari, B.P.; Joshi, P.G. Aging-Related Changes in Expression and Function of Glutamate Transporters in Rat Spinal Cord Astrocytes. *Neuroglia* **2023**, *4*, 290–306. <https://doi.org/10.3390/neuroglia4040020>

Academic Editor: Sergey Kasparov

Received: 27 September 2023

Revised: 16 November 2023

Accepted: 21 November 2023

Published: 24 November 2023



Copyright: © 2023 by the authors. Licensee MDPI, Basel, Switzerland. This article is an open access article distributed under the terms and conditions of the Creative Commons Attribution (CC BY) license (<https://creativecommons.org/licenses/by/4.0/>).

1. Introduction

Astrocytes are the abundant glial cells in the CNS [1,2]. They play numerous roles, including metabolic and trophic support, ion homeostasis, neurotransmitter buffering, and maintaining blood–brain barrier (BBB) integrity [3,4]. Astrocytes are the primary homeostatic cells of the central nervous system (CNS), possessing a diverse range of molecular programs and signaling pathways responsible for maintaining the health and functionality of neural tissue. By actively participating in the modulation of synaptic function, astrocytes contribute to the overall balance and stability of neural circuits, ensuring optimal brain function [5]. Recent studies provide evidence of a dynamic bidirectional interaction between astrocytes and neurons that regulate neuronal activity, thereby generating behavioral patterns [6].

Astrocytes play a crucial role in the central nervous system, particularly by absorbing surplus glutamate from the extracellular space that accumulates as a result of neuronal activity. Their delicate tendrils are optimally positioned to efficiently remove glutamate from synaptic regions. These astrocytic extensions are categorized into three types—branches, leaflets, and end feet—each with unique structural and functional attributes. Astrocytes in

the brain exhibit specialized interactions and functions through structural divisions. Their processes, distributed among synapses, establish contact with branches, leaflets, or both [7]. Dendritic spines, which are small protrusions, house neurotransmitter receptors. In contrast, the leaflets of astrocytic processes host key components like glutamate transporters. These specialized elements enable astrocytes to regulate neurotransmitter levels, maintain ion homeostasis, and actively participate in synaptic signaling [7,8].

Glutamate, the primary excitatory neurotransmitter in the central nervous system, is essential for healthy brain function. Elevated levels, however, can lead to adverse effects such as excitotoxicity, oxidative stress, and eventual neuronal death [9]. Astrocytes are crucial in regulating the concentration of extracellular glutamate [10]. Five types of excitatory amino acid transporters (EAAT1–5) collaborate to efficiently remove excess glutamate. EAAT1/GLAST and EAAT2/GLT1, primarily located on astrocytes, are key players, with EAAT2 handling nearly 90% of glutamate transport [10–14]. Despite EAAT2's dominance, EAAT1 significantly contributes to preventing excitotoxic damage to neurons [15]. EAAT3 is mainly found in neurons [16], while EAAT4 is specific to Purkinje cells, and EAAT5 is localized in the retina [17]. Dysfunctional astroglial activity due to changes in EAAT expression is linked to the exacerbation of glutamate-mediated excitotoxicity, playing a role in various neurological conditions, and is a factor in normal aging processes [18–24].

Aging is a key contributor to the advancement and worsening of neurodegenerative diseases, increasing the risk factor for neurodegeneration and worsening the severity of the disease [25–27]. It has been observed that aged individuals experience more severe forms of the disease and incomplete recovery after damage [28]. Reactive astrocytes, which undergo hypertrophy in response to pathological conditions, may exhibit maladaptive behaviors and become dysfunctional, worsening the existing pathology [29]. Moreover, molecular and cellular changes occurring during aging render neurons more susceptible to excitotoxicity, a phenomenon linked to neurodegenerative disorders, as supported by studies conducted on mouse models [30]. Given the late onset of numerous neurodegenerative diseases and the heightening of neurons to glutamate excitotoxicity, stemming from disrupted glutamate homeostasis [31–33], it becomes imperative to understand how astrocytes manage glutamate in the context of aging [21].

One of the emerging attributes of astrocytes in recent decades is their heterogeneity of structural and functional susceptibility, suggesting that astrocytes adapt according to the specific environment in which they exist [34]. For example, astrocytes in the VH express higher levels of inward rectifying K⁺ channel (Kir 4.1) compared to those in the DH [35,36]. Impaired potassium (K⁺) and glutamate homeostasis by astrocytes have been implicated in the pathology of various diseases such as amyotrophic lateral sclerosis (ALS) and Huntington's disease [37,38]. These findings highlight the importance of astrocytes in maintaining proper K⁺ and glutamate levels and suggest their involvement in the pathogenesis of certain neurodegenerative conditions. Additionally, in diseases such as ALS, motor neurons in the VH are preferentially susceptible, sparing other spinal sensory neurons, as shown by several studies, including ours [39–44]. Astrocytic characteristics vary not only between the DH and VH of the spinal cord but also among the laminae within the DH.

Numerous studies have conclusively demonstrated morphological and functional disparities between spinal sensory neurons in the DH and motor neurons in the VH. Despite this well-established divergence in neurons, limited exploration exists regarding analogous regional differences in astrocytes and how aging influences astrocytic characteristics. Astrocytes within the DH and VH likely exhibit distinctive functional roles due to their interactions with distinct neuronal types. Specifically, DH astrocytes may be more actively involved in processing sensory information, modulating pain, and facilitating synaptic transmission related to sensory input. Conversely, astrocytes in the VH may contribute to motor function and coordination.

To accomplish our research objectives, we employed the spinal cord as a model system, allowing us to scrutinize the astrocytic milieu encompassing motor neurons situated in the

VH and, concurrently, the spatially distinct but less vulnerable sensory neurons in the DH. This strategic approach enabled us to investigate these environments independently, avoiding any overlap and facilitating a focused exploration of the unique astrocytic attributes within each region. By adopting the spinal cord as our experimental model, we aimed to uncover nuanced details regarding the specialized roles and responses of astrocytes surrounding motor and sensory neurons. The separation of these environments not only enhances our understanding of astrocytic functions in distinct neuronal populations but also offers a comprehensive view of how astrocytes contribute to the overall homeostasis and susceptibility of neurons within these specific spinal cord regions.

Moreover, our investigation extends its scope to include age-related considerations. By examining astrocytic properties across various age groups, we aim to discern how aging influences the astrocytic environment, potentially shedding light on the mechanisms underlying age-associated changes in neural health and susceptibility to excitotoxicity. This multifaceted approach underscores the complexity of astrocytic interactions within the spinal cord, with implications for our understanding of neurodegenerative processes and the broader context of aging-related neurological conditions.

2. Materials and Methods

2.1. Materials

Polyclonal antibodies against EAAT1 and EAAT2 were obtained from Alomone Laboratories in Jerusalem, Israel. Secondary antibodies used were Alexa Fluor 488 goat anti-rabbit IgG, Alexa Fluor 633 goat anti-rabbit IgG, Alexa Fluor 633 goat anti-mouse IgG, and Alexa Fluor 488 goat anti-mouse IgG, all purchased from Molecular Probes, Invitrogen, Life Technologies in India. Neurochrom-cy3 conjugated, anti-GFAP-488 conjugated, Guinea pig anti-EAAT2, FITC goat anti-Guinea pig, and FITC rabbit anti-goat antibodies were obtained from Merck, Millipore India. Horseradish peroxidase (HRP) conjugated anti-rabbit and anti-mouse antibodies were obtained from Sigma Aldrich. L-glutamate was also purchased from Sigma Aldrich (St. Louis, MI, USA). S100 β was sourced from Santacruz Biotechnology. For Western blotting, antibodies against EAAT1, β -actin, and tubulin were obtained from Abcam. All other chemicals used were of analytical grade and were obtained from commercial sources.

2.2. Experimental Animals

Sprague Dawley rats both male and female of three age groups, namely juvenile (21 days), young adult (3 months), and old (20 months), were obtained from the Central Animal Research Facility of the National Institute of Mental Health and Neurosciences in Bangalore, India. All animal procedures were conducted in accordance with the guidelines of the institutional animal ethics committee. Briefly, rats were anesthetized using diethyl ether and subsequently decapitated. The study was conducted in accordance with the Declaration of Helsinki, and approved by the Institutional Animal Ethics Committee, CARF (Central Animal Research Facility) NIMHANS. (AEC/59/300(D)/B.P 2016).

2.3. Western Blotting

Whole-cell membrane fractions were prepared from the DH and VH of spinal cord tissue (lumbar region) isolated from different experimental groups. In brief, rats from different age groups were anesthetized and decapitated, and the spinal cord was quickly extracted using hydraulic extraction. An 11-gauge needle with a blunted tip, filled with Artificial CSF (aCSF), was inserted into the spinal canal near the L5 segment to a depth of 1 cm. The aCSF was forcefully injected to flush out the spinal cord. The cauda equina was identified, and the alignment of the spinal cord was adjusted accordingly, taking into account the rostral and caudal ends. The lumbar section of the spinal cord was isolated and placed in ice-cold HEPES buffer for 1–2 min. Subsequently, the spinal cord was sliced to a thickness of 800 μ m, and the DH was separated from the VH by making a horizontal slice at the level of the central canal, using a stereomicroscope. The separated DH and VH were

manually homogenized using a motor and piston homogenizer in lysis buffer (containing 10 mM Tris, 5 mM KCl, 1 mM DTT, 1 mM EGTA, and Complete Protease Inhibitor Cocktail (Abcam)), and the resulting cell lysate was sonicated.

The protein concentration was determined using the Lowry method [45], and the samples were then diluted 1:1 in sample treatment buffer (containing 25 mM Tris, 8% SDS, 40% glycerol, 0.05% bromophenol blue, and 20% β -mercaptoethanol). After denaturation by heating at 95 °C for 3–5 min, 100 μ g of protein was loaded into each lane of a 10% SDS-PAGE gel. Equal concentrations of proteins from both regions were loaded in each well and subjected to electrophoresis. Nonspecific binding sites were blocked with 5% non-fat milk, and the blots were incubated for 3 h at room temperature with rabbit polyclonal anti-EAAT1/anti-EAAT2 (1:200) and β -actin/tubulin (1:10,000). The blots were then probed with horseradish peroxidase-conjugated anti-rabbit (1:250) or anti-mouse (1:500) secondary antibodies using Super Signal[®] West Pico chemiluminescent substrate. The enhanced chemiluminescence signal was captured using a camera attached to a computer-assisted gel documentation system (Syngene, UK). Quantification of the band intensities was performed using Image J software version 1.54f (NIH, 9000 Rockville Pike, Bethesda, MD, USA).

2.4. Immunohistochemistry

Immunohistochemistry (IHC) was performed on free-floating spinal cord sections using the following primary antibodies: rabbit anti-EAAT1 (1:50), guinea pig anti-EAAT2 (1:1000), mouse anti-GFAP (1:400), and mouse anti-S100 β (1:100). Transcranial perfusion was carried out with chilled 0.9% saline, followed by 4% paraformaldehyde in PBS. The lumbar region of the spinal cord was extracted and kept in a 4 °C paraformaldehyde solution for 48 h, followed by transfer to PBS for an additional 24 h at 4 °C. Sections with a thickness of 70 μ m were prepared using a vibratome (Vibratome, 3000 Sectioning System). Antigen retrieval was performed by placing the sections in a solution of saline sodium citrate and formamide (1:1, volume ratio) with a pH of 6.4 for 2 h at 65 °C, using gentle shaking in a water bath. Non-specific antigen blocking and permeabilization were carried out by incubating the sections in PBS containing 5% bovine serum albumin, 5% goat serum, and 0.1% Triton X-100 at room temperature for 2 h. The sections were rinsed with PBS and then incubated in 100 μ L of PBS containing the primary antibody, 5% goat serum, and 5% bovine serum albumin for 12 h at 4 °C. After rinsing 5 times with PBS, Alexa fluor-488/633 conjugated or FITC conjugated secondary antibodies were added and incubated for 6 h in the dark at room temperature. The sections were thoroughly rinsed with PBS and mounted on gelatin-coated slides using a mounting solution consisting of 50% glycerol and 50% PBS (volume ratio). Images were acquired using a laser scanning confocal microscope (Olympus FV 1000, Olympus, Japan).

2.5. Quantification of Receptor Expression

For the quantification of receptor expression in immunofluorescence analysis of EAAT1 and EAAT2, images were acquired from the DH and VH of all three age groups. A minimum of 3 spinal cord sections from 3 different animals in each age group were selected for analysis. Image acquisition parameters were kept consistent for all age groups. Uniform-sized regions of interest (ROIs) were drawn in specific spinal cord areas of all the groups, and the average fluorescence intensity was obtained using Fluo-view software (Olympus, Japan). The VH percentages were calculated relative to the DH, which was normalized to 100% [46]. Data representing the mean \pm SEM were compared among the different experimental groups.

2.6. Quantification of Astrocytic Numerical Density and Coverage

For the quantification of astrocytic numerical density and coverage, S100 β -labeled spinal cord sections were used. The distribution of astrocytes in the DH, VH, and the entire spinal cord was analyzed and compared across different age groups. Cell counting and area analysis were performed on the acquired confocal microscope images using Im-

ageJ NIH image analysis software <http://rsb.info.nih.gov/ij/download.html> (accessed on 15 September 2023). For cell counting, the acquired images were converted into 8-bit binary images, and a threshold was set. The cells were then counted using an overlay of the original and binary images. For astrocytic coverage, the total area occupied by astrocytes was calculated using an automated binary thresholding method in ImageJ. The area covered by cells was measured and analyzed.

2.7. Acute Slice Preparation for Whole-Cell Patch-Clamp Recording

Transverse slices from the lumbar region of the spinal cord and coronal brain slices (300 μm) enclosing the hippocampus were prepared using a vibratome (Vibratome, 3000 Sectioning System) from deeply anesthetized Sprague Dawley rats of specific age groups. The brain/spinal cord was swiftly removed and placed in an ice-cold cutting buffer containing the following concentrations (in mM): 215 sucrose, 2.5 KCl, 1.25 NaH_2PO_4 , 0.5 CaCl_2 , 4 $\text{MgSO}_4 \cdot 7\text{H}_2\text{O}$, 26.2 NaHCO_3 , 1 ascorbate, equilibrated with a mixture of 95% O_2 and 5% CO_2 . The tissue was affixed to the slicing stage of a Leica vibratome. Subsequently, the slices were incubated in oxygenated minimum essential Eagle's medium (MEM) at room temperature (RT) for 1 h. Whole-cell patch-clamp recordings were then taken at RT using pipettes with resistances that typically ranging from 6 to 8 $\text{M}\Omega$ (P-2000, Sutter Instruments, Novato, CA, USA). The pipette solution consisted of the following concentrations (in mM): 145 potassium gluconate, 5 NaCl, 2 MgCl_2 , 10 HEPES, 0.2 EGTA. Astrocytes were visually identified and selected based on their size, location, and electrophysiological properties using infrared optics on an upright microscope (Eclipse E600-FN Nikon) (Figure S1). Inward currents were recorded at -70 mV [35] using Patchmaster software and an EPC10 amplifier (HEKA, Germany). The recorded data were filtered at 10 kHz (Bessel filter) and we compensated for C-fast and C-slow. L-glutamate (10 mM) was applied through superfusion without altering the perfusion rate and temperature.

2.8. Statistical Analysis

For statistical analysis, the OriginPro or SigmaPlot programs were employed, and the data are presented as mean \pm SEM. In experiments with two groups, an unpaired t-test was used to determine significance, while experiments with more than two groups were assessed using one-way ANOVA followed by the Fisher LSD post hoc test. The threshold for statistical significance was set at $p \leq 0.05$. In the figures, * represents $p \leq 0.05$, ** represents $p \leq 0.01$, and *** represents $p \leq 0.001$.

3. Results

3.1. Distinct Density and Morphology of Astrocytes in DH and VH of Rat Spinal Cord and Changes with Age

In the spinal cord, astrocytes ensheath motor and sensory neurons in the VH and DH, respectively. However, only motor neurons are highly vulnerable to glutamate excitotoxicity, and this vulnerability gradually increases with age [25,27]. Since astrocytes are the primary cells responsible for clearing extracellular glutamate, the higher vulnerability of motor neurons may underlie the structural and functional differences in DH and VH astrocytes.

To investigate this, we first assessed the numerical density of astrocytes with aging and whether any differential changes were occurring between DH and VH astrocytes. Using the astrocyte-specific marker S100 β in transverse spinal cord sections, we observed a remarkably lower number of astrocytes in the spinal cord with aging (Figure 1A,B). The density of astrocytes was highest in the juvenile spinal cord (260 ± 11 astrocytes/ mm^2 ; $n = 7$ rats), which decreased to over 50% in young adults (112 ± 7 astrocytes/ mm^2 ; $n = 5$ rats) and old age (96 ± 3 astrocytes/ mm^2 ; $n = 7$ rats) (Figure 1B).

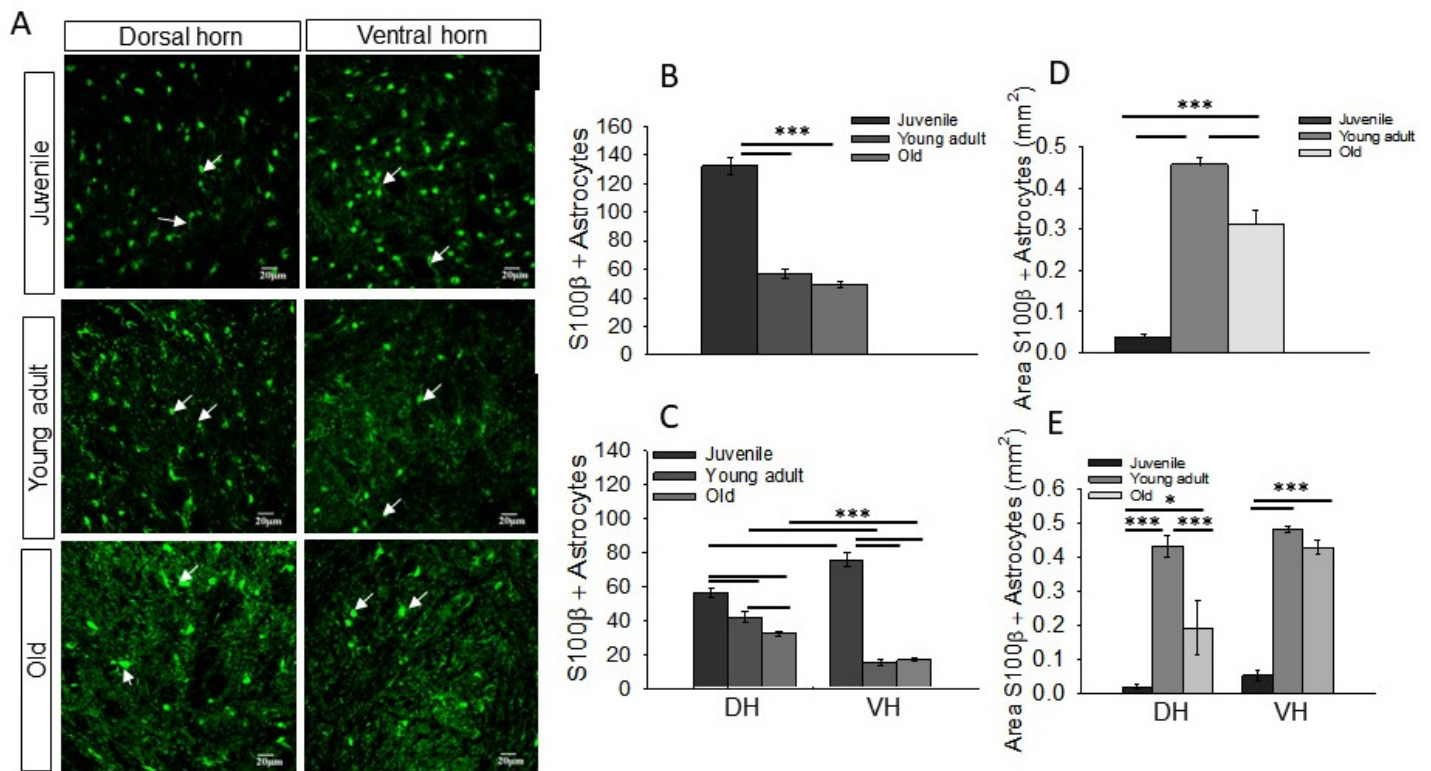


Figure 1. Density of astrocytes decreases with aging in spinal cord. (A) Representative images of immunohistochemistry showing S100 β -labeled astrocytes in dorsal horn and ventral horn of spinal cord, in three age groups. White arrows display astrocytes surrounding neuronal cell body. (B) Density of S100 β -labeled astrocytes significantly decreased with aging in spinal cord. (C) Density of astrocytes decreased in dorsal horn and ventral horn regions of spinal cord with aging. (D) Despite the number of astrocytes decreasing with age, the area acquired by astrocytes increased with age, and the area acquired by young adult astrocytes was the highest. (E) Graph shows same pattern in dorsal horn and ventral horn regions of spinal cord with least area acquired by juvenile astrocytes and maximum area acquired by young adult astrocytes. Data represent the mean \pm S.E.M., $n = 3\text{--}5$ rats (* $p \leq 0.05$; *** $p \leq 0.001$).

Next, to ascertain the differences in the astrocytic milieu of sensory and motor neurons with aging, we compared the density of S100 β -labeled astrocytes in the DH and VH of all age groups. In juvenile rats, the VH showed a higher density of astrocytes than the DH (VH 111 ± 4 astrocytes/mm², DH 149 ± 8 astrocytes/mm²; $n = 7$ rats) (Figure 1A,C). Furthermore, in the VH of young adults (DH 82 ± 6 astrocytes/mm², VH 29 ± 3 astrocytes/mm²; $n = 5$ rats) and old age groups (DH 63 ± 1 astrocytes/mm²; VH 32 ± 1.7 astrocytes/mm²; $n = 5$ rats), a significantly lower number of S100 β -positive astrocytes was observed compared to the DH (Figure 1C). Morphologically, astrocytic processes were less intricate in the juvenile group; however, S100 β immunofluorescence in the astrocytic processes appreciably increased in the young adult and old age groups, and the processes appeared more elaborate and profusely surrounded the neurons in both the DH and VH (Figure 1A, white arrows). These data suggest that the VH possesses a higher density of astrocytes than the DH at an early age; however, with aging, the total number of astrocytes decreases in both regions, with a more severe decline in the VH than the DH.

Since astrocytes undergo morphological maturation during development, which involves an increase in astrocytic arborizations and coverage [47], we examined whether a decline in astrocyte numbers affects overall glial coverage in the spinal cord. The juvenile age group, which exhibited a high numerical density of astrocytes (Figure 1B), showed the lowest glial coverage (Figure 1D, 0.037 ± 0.0 area/mm²; $n = 3$ rats). However, glial coverage increased approximately 14-fold in young adults (Figure 1D, 0.45 ± 0.02 area/mm²;

$n = 4$ rats) and subsequently decreased significantly in old age (Figure 1D, 0.31 ± 0.03 area/mm²; $n = 4$ rats). In the DH and VH, astrocytic coverage displayed a similar increase from the juvenile (Figure 1E, DH 0.02 ± 0.0 area/mm²; VH 0.05 ± 0.01 area/mm²; $n = 3$ rats) to young adult stages (Figure 1E, DH 0.43 ± 0.03 area/mm²; VH 0.48 ± 0.00 area/mm²; $n = 4$ rats), but only the DH exhibited a significant decline in the old age group (Figure 1E, DH 0.19 ± 0.07 area/mm²; VH 0.43 ± 0.02 area/mm²; $n = 4$ rats). These findings suggest that although the numerical density of astrocytes decreases with age, glial coverage appears to remain stable and only decreases in the DH during old age.

3.2. Change in Expression of Astrocytic Glutamate Transporters EAAT1 and EAAT2 in the Spinal Cord with Age

Next, we investigated whether astrocytes surrounding motor and sensory neurons exhibit different levels of glutamate transporter expression and whether this expression changes with aging. We began by analyzing the overall expression levels of EAAT1 and EAAT2 in the spinal cord through Western blot analysis using lumbar spinal cord tissue. As EAATs have been extensively studied in hippocampal astrocytes, we used hippocampal tissue as a positive control for transporter expression. Consistent with previous reports [48], we detected protein bands corresponding to EAAT1 and EAAT2 at approximately 60 kD and 65–67 kD, respectively (Figure 2A,B and Figure 3A,B).

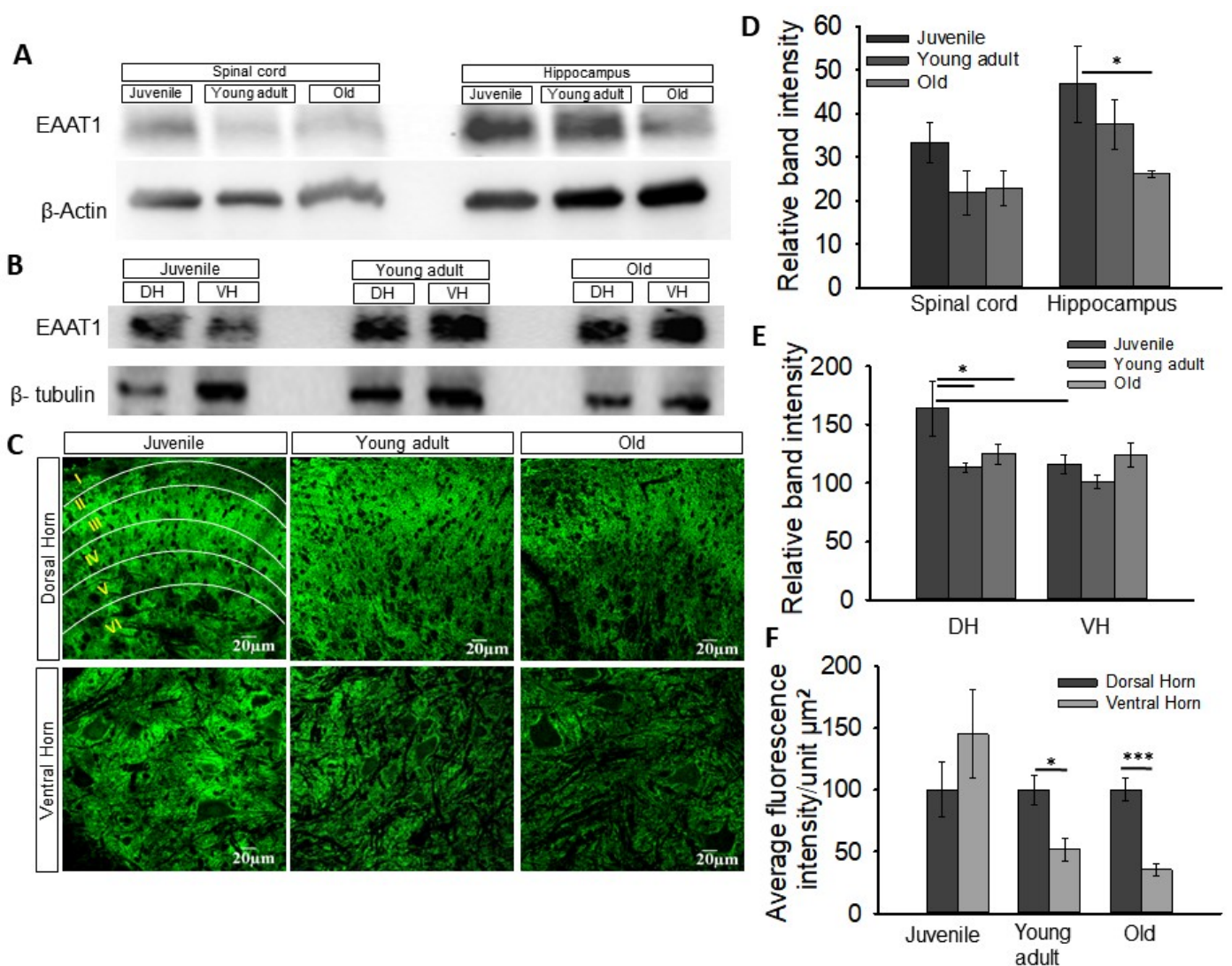


Figure 2. EAAT1 glutamate transporter expression decreased with aging in hippocampus of SD rat: (A,B) Representative Western blots show EAAT1, and beta-actin/beta-tubulin bands. (C) Confocal

image of a transverse section of rat lumbar spinal cord lamination DH is divided into laminae I-IV where only sensory neurons are present immunostained with EAAT1 astrocytic glutamate transporter. White lines represent boundaries of the dorsal horn laminae. Astrocytes from three age groups were immunostained with EAAT1 to assess effect of age in glutamate transporter expression. (D) Western blot analysis showed a decline in EAAT1 expression with aging in hippocampus, although there was no significant change in EAAT1 expression with age in spinal cord. (E) When comparing EAAT1 expression in different regions of spinal cord, EAAT1 showed a decline in its expression when dorsal horns of young adult and old rats were compared with those of juvenile rats. Also, the expression of EAAT1 in ventral horn of juvenile rats was lower than in ventral horns of young adult and old rats. (F) Evaluation of EAAT1 immunofluorescence in regions of spinal cord showed decreased EAAT1 expression in DH of young adult and old rats with no change in juvenile age group. Western blot data represent the mean \pm S.E.M. of $n = 3$ rats. IHC data represent the mean \pm S.E.M. of $n = 4$ rats (* $p \leq 0.05$; *** $p \leq 0.001$).

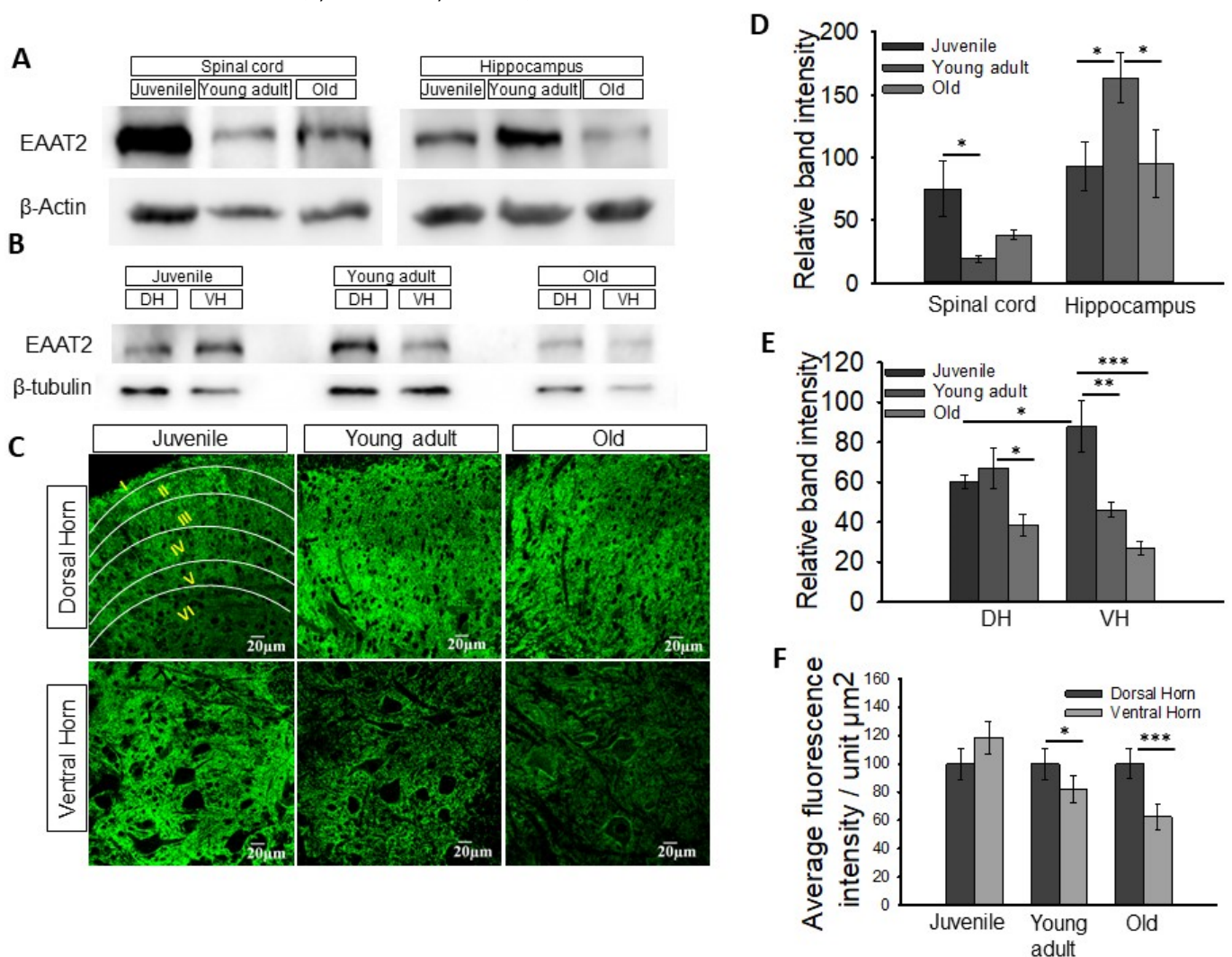


Figure 3. Most crucial glutamate transporter EAAT2 showed reduced expression with aging in regions of spinal cord. (A,B) Western blot images of EAAT1, and beta-actin/beta tubulin bands. (C) Immunostaining of astrocytes with EAAT2 transporter indicated the differential laminar expression pattern of transporter with intense expression in lamina II, III and IV of dorsal horn. Laminas

I, V and VI have low transporter expression (white lines), especially in young adult and old groups. (D) Spinal cord tissue had highest EAAT2 expression in juvenile age group followed by old and young adult groups. However, the positive control hippocampus portrayed highest EAAT2 levels in young adult rats. (E) The expression of EAAT2 decreased with maturing in both dorsal horn and ventral horn of spinal cord, with more prominent decrease in ventral horn. (F) Immunofluorescence data showed higher EAAT2 expression in DH for adult age groups as compared to VH astrocytes. Western blot data represent the mean \pm S.E.M. of $n = 3$ rats. IHC data represent the mean \pm S.E.M. of $n = 4$ rats (* $p \leq 0.05$; ** $p \leq 0.01$; *** $p \leq 0.001$).

In the spinal cord, EAAT1 expression was highest in the juvenile group (Figure 2A,D, 33 ± 4 , $n = 3$ rats) and decreased with age, although not significantly, in young adults (Figure 2A,D, 21 ± 5 , $n = 3$ rats) and old animals (Figure 2A,D, 22 ± 3 , $n = 3$ rats). Interestingly, the positive control hippocampus also exhibited the highest EAAT1 expression in juveniles, which significantly declined with age (Figure 2A,D, juvenile 46 ± 8 ; young adult 37 ± 5 ; old 26 ± 0.8 , $n = 3$ rats), suggesting age-related changes in EAAT1 expression independent of CNS region. Moreover, when comparing EAAT1 expression in the DH and VH, we found that the juvenile group showed significantly lower EAAT1 expression in the VH compared to the DH (Figure 2B,E, juvenile DH 164 ± 40 ; VH 116 ± 13 , $n = 3$ rats). As age progressed, EAAT1 expression significantly decreased in the DH, while the VH remained unchanged (Figure 2B,E, young adult DH 113 ± 7 , VH 101 ± 9 ; old DH 125 ± 14 , VH 124 ± 17 , $n = 3$ rats).

To further confirm the distribution and differential expression of EAAT1 with aging and in the DH and VH, we performed immunofluorescence analysis of EAAT1 in transverse sections of the spinal cord at the lumbar level. Expression was measured as the average fluorescence intensity/unit μm^2 . EAAT1 immunofluorescence exhibited a distinct pattern in the DH, with robust expression in rexed lamina II/III/IV, particularly in young adult and old animals (Figure 2C, outlined). In contrast, the VH showed relatively uniform expression, although in the young adult and old age groups, astrocytes appeared to surround the cell bodies of motor neurons. Also, in the young adult and old age groups, EAAT1 expression in the VH was significantly lower compared to the DH, with this difference being more prominent in old age (Figure 2C,F, young adult DH 100 ± 11 , VH 52 ± 9 ; old DH 100 ± 9 , VH 35 ± 4 , $n = 4$ rats). We did not observe any differences between the DH and VH in the juvenile group.

The expression of EAAT2, which is responsible for 90% of glutamate transport in astrocytes [49], declined with age in the spinal cord. The juvenile group exhibited a three-fold higher expression of EAAT2 (Figure 3D, 75 ± 21 , $n = 3$ rats) compared to the young adult group (Figure 3D, 19 ± 2 , $n = 3$ rats). However, there was no significant difference in EAAT2 expression between the old and young adult groups (Figure 3D, old 38 ± 4 , $n = 3$ rats). In the positive control hippocampus, EAAT2 expression was highest in the young adult group compared to the juvenile and old groups (Figure 3D, juvenile 93 ± 19 ; young adult 163 ± 20 ; old 95 ± 27 , $n = 3$ rats).

Furthermore, we compared the expression of EAAT2 in the DH and VH of the spinal cord. In the juvenile group, the VH exhibited higher EAAT2 expression than the DH (Figure 3E, DH 60 ± 3 ; VH 87 ± 12 , $n = 3$ rats). However, EAAT2 expression decreased with age, with significantly lower expression in the VH compared to the DH (Figure 3E, young adult DH 66 ± 10 , VH 46 ± 3 ; old DH 38 ± 5 , VH 26 ± 3 , $n = 3$ rats). Overall, these findings indicate a clear decrease in EAAT2 levels with age, particularly in the VH. However, the DH showed comparable EAAT2 expression between the juvenile and young adult groups, with old animals exhibiting the lowest EAAT2 expression (Figure 3E).

Immunohistochemistry data revealed similar EAAT2 expressions in the DH and VH of juvenile groups. However, the VH of the young adult and old groups exhibited lower EAAT2 expression compared to the DH (Figure 3C,F, old DH 100 ± 10 ; VH 62 ± 9 , $n = 4$ rats).

In summary, both EAAT1 and EAAT2 displayed distinct regional distribution patterns that varied to some extent among the three age groups (juvenile, young adult, and old). EAAT1 immunoreactivity was predominantly observed in lamina II compared to other laminae of the young adult and old spinal cords (Figure 2C, outlined). On the other hand, EAAT2 showed higher intensity in laminae III, IV, and V compared to laminae I and II, especially in young adult and old rats (Figure 3C, outlined). However, in juvenile spinal cord, EAAT2 appeared to be expressed uniformly from lamina I to IV. Both EAAT1 and EAAT2 were mostly uniformly distributed in the VH of the spinal cord, with more pronounced expression surrounding motor neurons (Figures 2C and 3C). Overall, the expression of EAAT1 and EAAT2 exhibited an overall decline in the spinal cord with aging, with VH astrocytes showing a more significant decline compared to DH astrocytes, suggesting a reduced capacity for glutamate uptake in VH astrocytes with age.

3.3. Glutamate Uptake in DH and VH Astrocytes with Aging

To assess glutamate uptake by astrocytes, we measured glutamate-induced currents in astrocytes of the DH and VH in ex vivo acute spinal cord slices, as well as in astrocytes of hippocampal slices. Astrocytes were identified and selected based on their morphology, size, location, and electrophysiological properties [50]. The resting membrane potential of astrocytes ranged from -68 mV to -70 mV ($n = 22$), while neurons exhibited a resting membrane potential of -60 mV to -63 mV ($n = 3$). When a 20 pA current was injected for 100 ms in the current clamp mode, neurons generated a train of action potentials, while astrocytes exhibited passive depolarization (Figure S2). We used glutamate current recordings from hippocampal astrocytes as a positive control.

For all the glutamate uptake current recordings in astrocytes, the membrane potential was held at -70 mV, and a 10 mM glutamate pulse was applied for 1 min using a superfusion system. Figure 4A presents representative traces of currents recorded from astrocytes in the DH, VH, and hippocampus across all three age groups. Astrocytes in the juvenile group displayed substantial glutamate uptake currents, which were comparable between the DH and VH (Figure 4B, DH 171 ± 33 pA; VH 155 ± 25 , $n = 12$ cells from 6 rats). We observed a significant decline in glutamate uptake currents in both DH and VH astrocytes of young adults (Figure 4B, DH 15 ± 4 pA; VH 13 ± 5 , $n = 5$ cells from 5 rats) and old rats (Figure 4B, DH 10 ± 5 pA; VH 10 ± 3 , $n = 5$ cells from 5 rats).

To serve as age-matched positive controls, we also measured glutamate uptake currents in hippocampal astrocytes from the CA1 region across all three age groups. Previous studies have reported a decline in astrocytic glutamate uptake currents during maturation [51]. Our data confirmed a substantial decrease in astrocytic glutamate uptake currents with aging in the hippocampus (Figure 4C, juvenile 335 ± 39 pA, $n = 6$ cells; young adult 153 ± 28 pA, $n = 4$ cells; old 110 ± 26 pA, $n = 6$ cells, from 4 rats). However, the glutamate uptake currents recorded in hippocampal astrocytes were much higher than those in spinal cord astrocytes. In the hippocampus, compared to the juvenile group, the higher age groups exhibited approximately a 67% decrease in glutamate uptake currents. In contrast, in the spinal cord, the glutamate uptake currents declined drastically (by 93%) in the higher age groups, with comparable uptake currents in young adult and old rats.

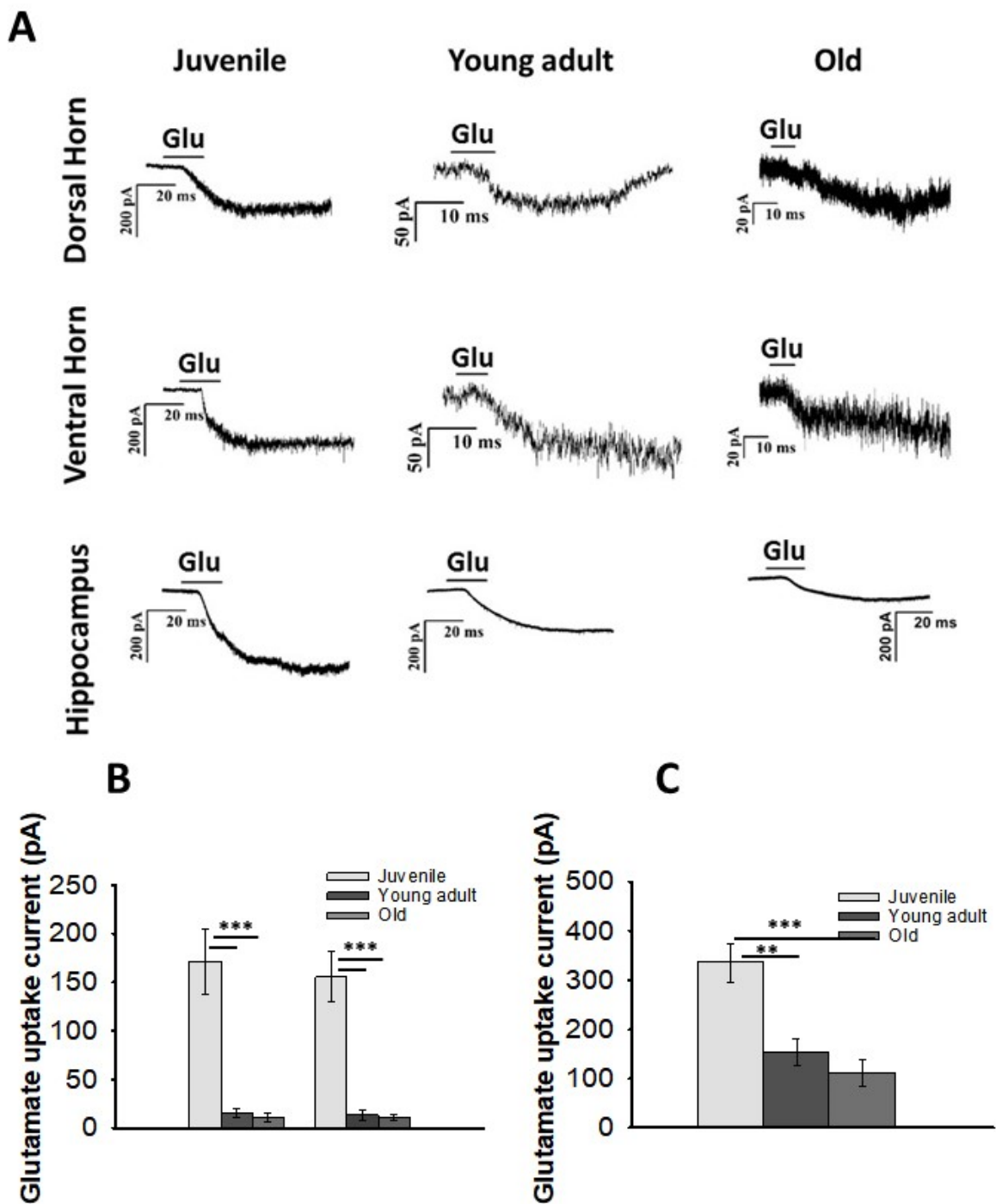


Figure 4. Glutamate transporter current in hippocampal and spinal astrocytes: **(A)** Representative astrocytic glutamate uptake current traces in spinal cord and hippocampal astrocytes with age. **(B)** Bar graph shows huge decline in average glutamate uptake current recorded from astrocytes of dorsal and ventral horn in spinal cord of young adult and old groups. **(C)** Hippocampal astrocytes demonstrated decline in glutamate uptake current with increasing age. Hippocampal astrocytes ($n = 5-8$); 15–30 days: dorsal horn ($n = 12$), ventral horn ($n = 12$); 2–3 months and 18–20 months: dorsal horn ($n = 5$), ventral horn ($n = 5$). Data represented as the mean \pm S.E.M. (** $p \leq 0.01$; *** $p \leq 0.001$).

4. Discussion

It is well-known that neuronal degeneration occurs during normal aging, and the onset of neurodegenerative disorders is typically associated with aging [25,52]. Glutamate-induced excitotoxicity has been implicated not only in the degeneration of neurons associated with aging but also in various neurodegenerative disorders. Recent studies have revealed that astrocytes undergo senescence and play a role in the aging process as well as in disease development [53,54]. Das and Svendsen (2015) reported that astrocytes derived from the spinal cords of aged rats and SOD193A mutant rats exhibit senescence phenotypes and have a reduced capacity to support motor neurons [30]. These studies were performed in astrocyte cultures derived from rat spinal cords, and their impact on the survival of co-cultured NSC34 motor neuron cells was assessed. However, most studies conducted in this field do not accurately replicate the neuron–astrocyte interaction as it occurs in vivo, and there is a significant lack of in vivo research in this area. In our study, our aim was to investigate the impact of aging on astrocyte properties in an in vivo setting, with a specific focus on the neuron–astrocyte interaction in the spinal cord. We examined the characteristics of astrocytes located in the VH and DH of the spinal cord, with particular emphasis on glutamate transporters.

Additionally, we examined the influence of aging on astrocyte characteristics. Our data demonstrate age-related changes in astrocytes that are considered unfavorable for neuronal survival, and these changes are generally more pronounced in the astrocytes surrounding motor neurons in the VH of the spinal cord. In the older age group, lumbar spinal cord slices showed a decreased density of S100 β -labeled astrocytes, suggesting a decline in astrocyte density with age. These changes were particularly prominent in the VH. Area analysis of S100 β -positive astrocytes revealed that astrocytic coverage increases with age, which could be attributed to age-related mild astrocytic hypertrophy without concurrent pathology [55]. The hypertrophy observed in aging does not mimic the astrogliosis seen in the young brain following injury [56–58]. Upon activation, astrocytes secrete factors that modulate neuronal survival, with activated astrocytes producing neurotrophic factors that promote neuronal growth [59]. The territorial domains of astrocytes in aged mice were found to be approximately 30% smaller compared to adult animals. Analysis of volume fraction measurements demonstrated significant dystrophy of the peripheral leaflet-like processes, which are important for astrocytic synaptic coverage. However, it is worth noting that the number of astrocytes remained unchanged in the aged mice compared to the adult animals [60,61].

In aged human brains, there are generally mild and diverse alterations in astrocyte morphology or GFAP levels. Studies conducted on rodents have documented region-specific and sometimes conflicting changes in aging astrocytes, including increased cellular volume and overlapping processes, as well as atrophy, elevated GFAP content, or even a decrease in the number of astrocytes positive for GFAP and GS markers [29,62]. With the normal aging process, a decline in physiological function, increased neuroinflammation, brain shrinkage, and memory deficits have been reported [63]. Astrocytes have been found to play a role in the heightened inflammatory state of the aged central nervous system (CNS). The age-related changes in astroglial morphology result in an increased presence of hypertrophic and reactive astrocytes in the aged brain.

Several studies have demonstrated that aged mouse cortical astrocytes exhibit upregulation of genes associated with immune responses, while the expression of glial fibrillary acidic protein (GFAP) and genes involved in neuroprotection and neuronal support is decreased. Researchers have also observed age-dependent shrinkage in astroglial peripheral processes [64]. Aging is characterized by intricate and region-specific changes in both gene expression and the structure of astrocytes. Notably, certain brain regions, such as the hippocampus, exhibit an increase in GFAP expression and alterations in the astroglial cytoskeleton. Moreover, the aging process is typically associated with an increased ratio of glutamate to glutamine in the brain, indicating possible irregularities in the operation of the glutamate (GABA)–glutamine shuttle. Furthermore, in aged rats (24–27 months old), there

is a notable decrease in the expression of astrocytic glutamate transporters and a reduction in the efficiency of glutamate uptake compared to young adults (3–5 months old). These collective findings significantly enhance our comprehension of the alterations observed in aged astrocytes and their potential significance in processes related to aging [51,64].

Many studies have been conducted on the expression and function of glutamate transporters in the brain, but limited information is available regarding glutamate transport in the spinal cord. Furuta et al. (1997) investigated the expression of glutamate transporters in the central nervous system (CNS) during development and demonstrated that the expression of glutamate transporter subtypes changes during development, from embryonic day 15 to postnatal day 24 [65]. However, there are no reports on the expression of glutamate transporter proteins and their activity in the spinal cord of aged animals. Our data reveal a decline in glutamate transporter expression with aging in spinal cord astrocytes, particularly in the VH. The glial glutamate transporters EAAT1 and EAAT2 were observed to be expressed in both regions of the spinal cord in all age groups, but their expression significantly declined with aging. Additionally, the expression of both transporters was notably lower in the VH compared to the DH.

We measured glutamate-induced currents in astrocytes using the whole-cell patch clamp technique. Astrocytes in the juvenile group exhibited substantial glutamate uptake currents, albeit significantly lower than the glutamate uptake currents observed in the age-matched hippocampus. The glutamate uptake current was suppressed with aging, both in the hippocampus and the spinal cord. A decrease in the expression of glial glutamate transporters EAAT1 and EAAT2, as well as reduced glutamate uptake, was observed in the aged Sprague Dawley rat hippocampus. Similar findings have been reported in the striatum of the hippocampus, where glutamate clearance was compromised in the aged brain [48]. These variances in glutamate uptake currents may indicate either varying demands on glutamate homeostasis or undermined glutamate management potential with aging. Extensive proof suggests that glutamate uptake into astrocytes occurs through sodium-dependent excitatory amino acid transporters (EAATs), and studies have revealed that the larger portion of glutamate uptake is mediated by astrocytic glutamate transporter EAAT2 [10,13]. Interestingly, the decline in glutamate uptake current was more evident in the spinal cord. Compared to the juvenile group, the uptake current was at least ten times lower in young adult and older rats (Figure 4). Nonetheless, appreciable glutamate transporter expression was observed in the old age group. Several studies have demonstrated that an increase in intracellular glutamate and sodium ions leads to a decrease in glutamate transporter currents in astrocytes [66]. The activity of glutamine synthase (GS) in astrocytes dynamically regulates intracellular glutamate concentration [67], thus influencing glutamate transport across the membrane. Souza et al. (2015) reported a decrease in astrocytic GS activity in adult and old rats [68]. However, we measured glutamate uptake currents under whole-cell voltage clamp conditions, and the intracellular glutamate concentrations under the given experimental conditions would be similar in all age groups. Therefore, the observed decline in glutamate uptake current in the old age group is less likely to be attributed to the factors mentioned above.

In essence, our study offers compelling evidence pointing towards impaired glutamate management by astrocytes as individuals age. The well-established role of astrocytes in maintaining optimal extracellular glutamate levels at the synaptic cleft becomes particularly pertinent. Our findings highlight a compromised glutamate uptake capacity in aging astrocytes, as evidenced by both a decline in the expression of relevant transporters and a decrease in overall glutamate uptake efficiency with advancing age. Furthermore, our study unveils distinctive morphological and functional characteristics of astrocytes within the DH and VH of the spinal cord. Given our observation of reduced astrocytic glutamate transporter expression, particularly notable in the VH, further investigations are warranted to fully elucidate the implications of these changes.

Supplementary Materials: The following supporting information can be downloaded at: <https://www.mdpi.com/article/10.3390/neuroglia4040020/s1>, Figure S1. An image of a dye filled patched astrocyte (Alexa 488 channel, 20–30 µm deep in the slice, single optical section. Figure S2. Comparison of electrophysiological properties of neurons and astrocytes in rat spinal cord slice. Figure S3. Morphology of astrocytes in spinal cord with age progression.

Author Contributions: S.S.: conceptualization, conducted experiments, methodology, data curation, visualization, investigation, validation, writing the original draft and reviewing; B.P.T.: methodology, writing, reviewing, editing; P.G.J.: supervision, conceptualization, visualization, methodology, validation. All authors have read and agreed to the published version of the manuscript.

Funding: This study was supported by the Department of Science and Technology, New Delhi, India. S.S. received a fellowship from the Department of Science and Technology, Government of India.

Institutional Review Board Statement: The study was conducted in accordance with the Declaration of Helsinki, and approved by the Institutional Animal Ethics Committee, CARF (Central Animal Research Facility) NIMHANS. (AEC/59/300(D)/B.P 2016).

Informed Consent Statement: Not applicable.

Data Availability Statement: The data that support the findings of this study are available on request from the corresponding author. The data are not publicly available due to privacy and ethical restrictions.

Acknowledgments: Animal facility: Central Animal Research Facility, National Institute of Mental Health & Neurosciences, Bangalore, India.

Conflicts of Interest: The authors declare that they have no known competing financial interests or personal relationships that could have appeared to influence the work reported in this paper.

Abbreviations

DH: dorsal horn, VH: ventral horn, CA1: cornu ammonis 1, EAAT1: excitatory amino acid transporter 1, EAAT2: excitatory amino acid transporter 1.

References

1. Verkhratsky, A.; Nedergaard, M. Physiology of Astroglia. *Physiol. Rev.* **2018**, *98*, 239–389. [[CrossRef](#)] [[PubMed](#)]
2. Belanger, M.; Allaman, I.; Magistretti, P.J. Magistretti, Brain energy metabolism: Focus on astrocyte-neuron metabolic cooperation. *Cell Metab.* **2011**, *14*, 724–738. [[CrossRef](#)] [[PubMed](#)]
3. Kim, Y.; Park, J.; Choi, Y.K. The Role of Astrocytes in the Central Nervous System Focused on BK Channel and Heme Oxygenase Metabolites: A Review. *Antioxidants* **2019**, *8*, 121. [[CrossRef](#)] [[PubMed](#)]
4. Liddel, S.A.; Guttenplan, K.A.; Clarke, L.E.; Bennett, F.C.; Bohlen, C.J.; Schirmer, L.; Bennett, M.L.; Münch, A.E.; Chung, W.-S.; Peterson, T.C.; et al. Neurotoxic reactive astrocytes are induced by activated microglia. *Nature* **2017**, *541*, 481–487. [[CrossRef](#)] [[PubMed](#)]
5. Augusto-Oliveira, M.; Arrifano, G.P.; Takeda, P.Y.; Lopes-Araujo, A.; Santos-Sacramento, L.; Anthony, D.C.; Verkhratsky, A.; Crespo-Lopez, M.E. Astroglia-specific contributions to the regulation of synapses, cognition and behaviour. *Neurosci. Biobehav. Rev.* **2020**, *118*, 331–357. [[CrossRef](#)] [[PubMed](#)]
6. Nagai, J.; Yu, X.; Papouin, T.; Cheong, E.; Freeman, M.R.; Monk, K.R.; Hastings, M.H.; Haydon, P.G.; Rowitch, D.; Shaham, S.; et al. Behaviorally consequential astrocytic regulation of neural circuits. *Neuron* **2021**, *109*, 576–596. [[CrossRef](#)] [[PubMed](#)]
7. Semyanov, A.; Verkhratsky, A. Astrocytic processes: From tripartite synapses to the active milieu. *Trends Neurosci.* **2021**, *44*, 781–792. [[CrossRef](#)]
8. Murphy-Royal, C.; Dupuis, J.P.; Varela, J.A.; Panatier, A.; Pinson, B.; Baufreton, J.; Groc, L.; Oliet, S.H. Surface diffusion of astrocytic glutamate transporters shapes synaptic transmission. *Nat. Neurosci.* **2015**, *18*, 219–226. [[CrossRef](#)]
9. Iovino, L.; Tremblay, M.E.; Civiero, L. Glutamate-induced excitotoxicity in Parkinson's disease: The role of glial cells. *J. Pharmacol. Sci.* **2020**, *144*, 151–164. [[CrossRef](#)]
10. Anderson, C.M.; Swanson, R.A. Astrocyte glutamate transport: Review of properties, regulation, and physiological functions. *Glia* **2000**, *32*, 1–14. [[CrossRef](#)]
11. Pines, G.; Danbolt, N.C.; Bjørås, M.; Zhang, Y.; Bendahan, A.; Eide, L.; Koepsell, H.; Storm-Mathisen, J.; Seeberg, E.; Kanner, B.I. Cloning and expression of a rat brain L-glutamate transporter. *Nature* **1992**, *360*, 464–467. [[CrossRef](#)] [[PubMed](#)]
12. Storck, T.; Schulte, S.; Hofmann, K.; Stoffel, W. Structure, expression, and functional analysis of a Na(+)-dependent glutamate/aspartate transporter from rat brain. *Proc. Natl. Acad. Sci. USA* **1992**, *89*, 10955–10959. [[CrossRef](#)] [[PubMed](#)]

13. Lehre, K.P.; Danbolt, N.C. The number of glutamate transporter subtype molecules at glutamatergic synapses: Chemical and stereological quantification in young adult rat brain. *J. Neurosci.* **1998**, *18*, 8751–8757. [[CrossRef](#)] [[PubMed](#)]
14. Ortega, A. glutamate transporters: Critical components of glutamatergic transmission neuropharmacology. *Neuropharmacology* **2021**, *192*, 108602.
15. Pajarillo, E.; Rizor, A.; Lee, J.; Aschner, M.; Lee, E. The role of astrocytic glutamate transporters GLT-1 and GLAST in neurological disorders: Potential targets for neurotherapeutics. *Neuropharmacology* **2019**, *161*, 107559. [[CrossRef](#)] [[PubMed](#)]
16. Holmseth, S.; Dehnes, Y.; Huang, Y.H.; Follin-Arbelet, V.V.; Grutle, N.J.; Mylonakou, M.N.; Plachez, C.; Zhou, Y.; Furness, D.N.; Bergles, D.E.; et al. The density of EAAC1 (EAAT3) glutamate transporters expressed by neurons in the mammalian CNS. *J. Neurosci.* **2012**, *32*, 6000–6013. [[CrossRef](#)] [[PubMed](#)]
17. Magi, S.; Piccirillo, S.; Amoroso, S.; Lariccia, V. Excitatory Amino Acid Transporters (EAATs): Glutamate Transport and Beyond. *Int. J. Mol. Sci.* **2019**, *20*, 5674. [[CrossRef](#)] [[PubMed](#)]
18. Alcoreza, O.B.; Patel, D.C.; Tewari, B.P.; Sontheimer, H. Dysregulation of Ambient Glutamate and Glutamate Receptors in Epilepsy: An Astrocytic Perspective. *Front. Neurol.* **2021**, *12*, 652159. [[CrossRef](#)]
19. Peterson, A.R.; Binder, D.K. Astrocyte Glutamate Uptake and Signaling as Novel Targets for Antiepileptogenic Therapy. *Front. Neurol.* **2020**, *11*, 1006. [[CrossRef](#)]
20. Verhoog, Q.P.; Holtman, L.; Aronica, E.; van Vliet, E.A. Astrocytes as Guardians of Neuronal Excitability: Mechanisms Underlying Epileptogenesis. *Front. Neurol.* **2020**, *11*, 591690. [[CrossRef](#)]
21. Mattson, M.P.; Magnus, T. Ageing and neuronal vulnerability. *Nat. Rev. Neurosci.* **2006**, *7*, 278–294. [[CrossRef](#)] [[PubMed](#)]
22. Farrand, A.Q.; Gregory, R.A.; Scofield, M.D.; Helke, K.L.; Boger, H.A. Effects of aging on glutamate neurotransmission in the substantia nigra of Gdnf heterozygous mice. *Neurobiol. Aging* **2015**, *36*, 1569–1576. [[CrossRef](#)] [[PubMed](#)]
23. Lewerenz, J.; Maher, P. Chronic Glutamate Toxicity in Neurodegenerative Diseases-What is the Evidence? *Front. Neurosci.* **2015**, *9*, 469. [[CrossRef](#)] [[PubMed](#)]
24. Bronzuoli, M.R.; Facchinetti, R.; Valenza, M.; Cassano, T.; Steardo, L.; Scuderi, C. Astrocyte Function Is Affected by Aging and Not Alzheimer's Disease: A Preliminary Investigation in Hippocampi of 3xTg-AD Mice. *Front. Pharmacol.* **2019**, *10*, 644. [[CrossRef](#)]
25. Wyss-Coray, T. neurodegeneration and brain rejuvenation. *Nature* **2016**, *539*, 180–186. [[CrossRef](#)] [[PubMed](#)]
26. Broussalis, E.; Grininger, S.; Kunz, A.B.; Killer-Oberpfalzer, M.; Haschke-Becher, E.; Hartung, H.-P.; Kraus, J. Late age onset of amyotrophic lateral sclerosis is often not considered in elderly people. *Acta Neurol. Scand.* **2018**, *137*, 329–334. [[CrossRef](#)] [[PubMed](#)]
27. Le Gall, L.; Connolly, O.; Vijayakumar, U.G.; Duddy, W.J.; Duguez, S. Molecular and Cellular Mechanisms Affected in ALS. *J. Pers. Med.* **2020**, *10*, 101. [[CrossRef](#)] [[PubMed](#)]
28. Mayne, K.; White, J.A.; McMurrin, C.E.; Rivera, F.J.; de la Fuente, A.G. Aging and Neurodegenerative Disease: Is the Adaptive Immune System a Friend or Foe? *Front. Aging Neurosci.* **2020**, *12*, 572090. [[CrossRef](#)]
29. Campuzano, O.; Castillo-Ruiz, M.M.; Acarin, L.; Castellano, B.; Gonzalez, B. Increased levels of proinflammatory cytokines in the aged rat brain attenuate injury-induced cytokine response after excitotoxic damage. *J. Neurosci. Res.* **2009**, *87*, 2484–2497. [[CrossRef](#)]
30. Das, M.M.; Svendsen, C.N. Astrocytes show reduced support of motor neurons with aging that is accelerated in a rodent model of ALS. *Neurobiol. Aging* **2015**, *36*, 1130–1139. [[CrossRef](#)]
31. Foran, E.; Trotti, D.; Abousaab, A.; Warsi, J.; Elvira, B.; Lang, F.; Alesutan, I.; Gasparini, C.F.; Sutherland, H.G.; Maher, B.; et al. Glutamate transporters and the excitotoxic path to motor neuron degeneration in amyotrophic lateral sclerosis. *Antioxid. Redox Signal.* **2009**, *11*, 1587–1602. [[CrossRef](#)] [[PubMed](#)]
32. King, A.E.; Woodhouse, A.; Kirkcaldie, M.T.; Vickers, J.C. Excitotoxicity in ALS: Overstimulation, or overreaction? *Exp. Neurol.* **2016**, *275 Pt 1*, 162–171. [[CrossRef](#)] [[PubMed](#)]
33. Gasiorowska, A.; Wydrych, M.; Drapich, P.; Zadrozny, M.; Steczkowska, M.; Niewiadomski, W.; Niewiadomska, G. The Biology and Pathobiology of Glutamatergic, Cholinergic, and Dopaminergic Signaling in the Aging Brain. *Front. Aging Neurosci.* **2021**, *13*, 654931. [[CrossRef](#)] [[PubMed](#)]
34. Clarke, B.E.; Taha, D.M.; Tyzack, G.E.; Patani, R. Regionally encoded functional heterogeneity of astrocytes in health and disease: A perspective. *Glia* **2021**, *69*, 20–27. [[CrossRef](#)] [[PubMed](#)]
35. Olsen, M.L.; Campbell, S.L.; Sontheimer, H.; Shih, E.K.; Robinson, M.B.; Verkhatsky, A.; Nedergaard, M.; Hibino, H.; Inanobe, A.; Furutani, K.; et al. Differential distribution of Kir4.1 in spinal cord astrocytes suggests regional differences in K⁺ homeostasis. *J. Neurophysiol.* **2007**, *98*, 786–793. [[CrossRef](#)] [[PubMed](#)]
36. Kelley, K.W.; Ben Haim, L.; Schirmer, L.; Tyzack, G.E.; Tolman, M.; Miller, J.G.; Tsai, H.-H.; Chang, S.M.; Molofsky, A.V.; Yang, Y.; et al. Kir4.1-Dependent Astrocyte-Fast Motor Neuron Interactions Are Required for Peak Strength. *Neuron* **2018**, *98*, 306.e7–319.e7. [[CrossRef](#)] [[PubMed](#)]
37. Phatnani, H.; Maniatis, T. Astrocytes in neurodegenerative disease. *Cold Spring Harb. Perspect. Biol.* **2015**, *7*, a020628. [[CrossRef](#)]
38. Tong, X.; Ao, Y.; Faas, G.C.; Nwaobi, S.E.; Xu, J.; Hausteiner, M.D.; Anderson, M.A.; Mody, I.; Olsen, M.L.; Sofroniew, M.V.; et al. Astrocyte Kir4.1 ion channel deficits contribute to neuronal dysfunction in Huntington's disease model mice. *Nat. Neurosci.* **2014**, *17*, 694–703. [[CrossRef](#)]
39. Mayhew, J.; Callister, R.; Walker, F.; Smith, D.; Graham, B. Aging alters signaling properties in the mouse spinal dorsal horn. *Mol. Pain* **2019**, *15*, 1744806919839860. [[CrossRef](#)]

40. Carriedo, S.G.; Sensi, S.L.; Yin, H.Z.; Weiss, J.H. AMPA exposures induce mitochondrial Ca(2+) overload and ROS generation in spinal motor neurons in vitro. *J. Neurosci.* **2000**, *20*, 240–250. [[CrossRef](#)]
41. Joshi, D.C.; Singh, M.; Krishnamurthy, K.; Joshi, P.G.; Joshi, N.B. AMPA induced Ca²⁺ influx in motor neurons occurs through voltage gated Ca²⁺ channel and Ca²⁺ permeable AMPA receptor. *Neurochem. Int.* **2011**, *59*, 913–921. [[CrossRef](#)] [[PubMed](#)]
42. Joshi, D.C.; Tewari, B.P.; Singh, M.; Joshi, P.G.; Joshi, N.B. AMPA receptor activation causes preferential mitochondrial Ca²⁺ load and oxidative stress in motor neurons. *Brain Res.* **2015**, *1616*, 1–9. [[CrossRef](#)] [[PubMed](#)]
43. Sen, I.; Joshi, D.C.; Joshi, P.G.; Joshi, N.B. NMDA and non-NMDA receptor-mediated differential Ca²⁺ load and greater vulnerability of motor neurons in spinal cord cultures. *Neurochem. Int.* **2008**, *52*, 247–255. [[CrossRef](#)] [[PubMed](#)]
44. Van Den Bosch, L.; Van Damme, P.; Bogaert, E.; Robberecht, W. The role of excitotoxicity in the pathogenesis of amyotrophic lateral sclerosis. *Biochim. Biophys. Acta BBA-Mol. Basis Dis.* **2006**, *1762*, 1068–1082. [[CrossRef](#)] [[PubMed](#)]
45. Lowry, O.H.; Rosebrough, N.J.; Farr, A.L.; Randall, R.J. Protein measurement with the Folin phenol reagent. *J. Biol. Chem.* **1951**, *193*, 265–275. [[CrossRef](#)] [[PubMed](#)]
46. Jones, J.; Estirado, A.; Redondo, C.; Martinez, S. Stem cells from wildtype and Friedreich's ataxia mice present similar neuroprotective properties in dorsal root ganglia cells. *PLoS ONE* **2013**, *8*, e62807. [[CrossRef](#)] [[PubMed](#)]
47. Torres-Ceja, B.; Olsen, M.L. A closer look at astrocyte morphology: Development, heterogeneity, and plasticity at astrocyte leaflets. *Curr. Opin. Neurobiol.* **2022**, *74*, 102550. [[CrossRef](#)] [[PubMed](#)]
48. Nickell, J.; Salvatore, M.F.; Pomerleau, F.; Apparsundaram, S.; Gerhardt, G.A. Reduced plasma membrane surface expression of GLAST mediates decreased glutamate regulation in the aged striatum. *Neurobiol. Aging* **2007**, *28*, 1737–1748. [[CrossRef](#)]
49. Sheldon, A.L.; Robinson, M.B. The role of glutamate transporters in neurodegenerative diseases and potential opportunities for intervention. *Neurochem. Int.* **2007**, *51*, 333–355. [[CrossRef](#)]
50. McNeill, J.; Rudyk, C.; Hildebrand, M.E.; Salmaso, N. Ion Channels and Electrophysiological Properties of Astrocytes: Implications for Emergent Stimulation Technologies. *Front. Cell. Neurosci.* **2021**, *15*, 644126. [[CrossRef](#)]
51. Potier, B.; Billard, J.; Rivière, S.; Sinet, P.; Denis, I.; Champeil-Potokar, G.; Grinvald, B.; Jouvenceau, A.; Kollen, M.; Dutar, P. Reduction in glutamate uptake is associated with extrasynaptic NMDA and metabotropic glutamate receptor activation at the hippocampal CA1 synapse of aged rats. *Aging Cell* **2010**, *9*, 722–735. [[CrossRef](#)] [[PubMed](#)]
52. Azam, S.; Haque, E.; Balakrishnan, R.; Kim, I.-S.; Choi, D.-K. The Ageing Brain: Molecular and Cellular Basis of Neurodegeneration. *Front. Cell Dev. Biol.* **2021**, *9*, 683459. [[CrossRef](#)] [[PubMed](#)]
53. Salminen, A.; Ojala, J.; Kaarniranta, K.; Haapasalo, A.; Hiltunen, M.; Soininen, H. Astrocytes in the aging brain express characteristics of senescence-associated secretory phenotype. *Eur. J. Neurosci.* **2011**, *34*, 3–11. [[CrossRef](#)] [[PubMed](#)]
54. Chinta, S.J.; Lieu, C.A.; DeMaria, M.; Laberge, R.-M.; Campisi, J.; Andersen, J.K. Environmental stress, ageing and glial cell senescence: A novel mechanistic link to Parkinson's disease? *J. Intern. Med.* **2013**, *273*, 429–436. [[CrossRef](#)] [[PubMed](#)]
55. Finch, C.E. Neurons, glia, and plasticity in normal brain aging. *Neurobiol. Aging* **2003**, *24* Suppl. S1, S123–S127; discussion S131. [[CrossRef](#)] [[PubMed](#)]
56. Faulkner, J.R.; Herrmann, J.E.; Woo, M.J.; Tansey, K.E.; Doan, N.B.; Sofroniew, M.V. Reactive astrocytes protect tissue and preserve function after spinal cord injury. *J. Neurosci.* **2004**, *24*, 2143–2155. [[CrossRef](#)] [[PubMed](#)]
57. Sofroniew, M.V. Reactive astrocytes in neural repair and protection. *Neuroscientist* **2005**, *11*, 400–407. [[CrossRef](#)]
58. Voskuhl, R.R.; Peterson, R.S.; Song, B.; Ao, Y.; Morales, L.B.J.; Tiwari-Woodruff, S.; Sofroniew, M.V. Reactive astrocytes form scar-like perivascular barriers to leukocytes during adaptive immune inflammation of the CNS. *J. Neurosci.* **2009**, *29*, 11511–11522. [[CrossRef](#)]
59. Albrecht, P.J.; Dahl, J.P.; Stoltzfus, O.K.; Levenson, R.; Levison, S.W. Ciliary neurotrophic factor activates spinal cord astrocytes, stimulating their production and release of fibroblast growth factor-2, to increase motor neuron survival. *Exp. Neurol.* **2002**, *173*, 46–62. [[CrossRef](#)]
60. Verkhatsky, A.; Lazareva, N.; Semyanov, A. Glial decline and loss of homeostatic support rather than inflammation defines cognitive aging. *Neural Regen. Res.* **2022**, *17*, 565–566. [[CrossRef](#)]
61. Popov, A.; Brazhe, A.; Denisov, P.; Sutyagina, O.; Li, L.; Lazareva, N.; Verkhatsky, A.; Semyanov, A. Astrocyte dystrophy in ageing brain parallels impaired synaptic plasticity. *Aging Cell* **2021**, *20*, e13334. [[CrossRef](#)] [[PubMed](#)]
62. Escartin, C.; Galea, E.; Lakatos, A.; O'Callaghan, J.P.; Petzold, G.C.; Serrano-Pozo, A.; Steinhauser, C.; Volterra, A.; Carmignoto, G.; Agarwal, A.; et al. Reactive astrocyte nomenclature, definitions, and future directions. *Nat. Neurosci.* **2021**, *24*, 312–325. [[CrossRef](#)] [[PubMed](#)]
63. Esiri, M.M. Ageing and the brain. *J. Pathol.* **2007**, *211*, 181–187. [[CrossRef](#)] [[PubMed](#)]
64. Verkhatsky, A.; Augusto-Oliveira, M.; Pivoriūnas, A.; Popov, A.; Brazhe, A.; Semyanov, A. Astroglial asthenia and loss of function, rather than reactivity, contribute to the ageing of the brain. *Pflügers Arch. Eur. J. Physiol.* **2021**, *473*, 753–774. [[CrossRef](#)] [[PubMed](#)]
65. Furuta, A.; Rothstein, J.D.; Martin, L.J. Glutamate transporter protein subtypes are expressed differentially during rat CNS development. *J. Neurosci.* **1997**, *17*, 8363–8375. [[CrossRef](#)] [[PubMed](#)]
66. Danbolt, N.C. Glutamate uptake. *Prog. Neurobiol.* **2001**, *65*, 1–105. [[CrossRef](#)] [[PubMed](#)]

67. Schousboe, A.; Scafidi, S.; Bak, L.K.; Waagepetersen, H.S.; McKenna, M.C. Glutamate metabolism in the brain focusing on astrocytes. *Adv. Neurobiol.* **2014**, *11*, 13–30. [[CrossRef](#)]
68. Souza, D.G.; Bellaver, B.; Raupp, G.S.; Souza, D.O.; Quincozes-Santos, A. Astrocytes from adult Wistar rats aged in vitro show changes in glial functions. *Neurochem. Int.* **2015**, *90*, 93–97. [[CrossRef](#)]

Disclaimer/Publisher’s Note: The statements, opinions and data contained in all publications are solely those of the individual author(s) and contributor(s) and not of MDPI and/or the editor(s). MDPI and/or the editor(s) disclaim responsibility for any injury to people or property resulting from any ideas, methods, instructions or products referred to in the content.